Earth and Planetary Science Letters xxx (2011) xxx–xxx

Contents lists available at ScienceDirect

Earth and Planetary Science Letters

journal homepage: www.elsevier.com/locate/epsl

Modeling the surface mass-balance response of the Laurentide Ice Sheet to Bølling warming and its contribution to Meltwater Pulse 1A

Anders E. Carlson [a,b,*], David J. Ullman [a], Faron S. Anslow [c], Feng He [b], Peter U. Clark [d], Zhengyu Liu [b], Bette L. Otto-Bliesner [e]

[a] Department of Geoscience, University of Wisconsin, Madison, WI 53706, USA
[b] Center for Climatic Research, University of Wisconsin, Madison, WI 53706, USA
[c] Pacific Climate Impacts Consortium, University of Victoria, Victoria, BC, Canada V8W 2Y2
[d] Department of Geosciences, Oregon State University, Corvallis, OR 97331, USA
[e] Climate and Global Dynamics Division, National Center for Atmospheric Research, Boulder, CO 80307, USA

ARTICLE INFO

Article history:
Accepted 10 July 2011
Available online xxxx

Keywords:
Laurentide Ice Sheet
surface mass-balance
sea-level rise
Bølling warm period
Meltwater Pulse 1A

ABSTRACT

Meltwater Pulse (MWP) 1A occurred ~14.5–14 ka and is the largest abrupt rise in sea level (10–20 m of sea-level rise) of the last deglaciation. The timing of MWP-1A is coincident with or shortly follows the abrupt warming of the North Atlantic region into the Bølling warm period, which could have triggered a large Laurentide Ice Sheet (LIS) contribution to MWP-1A. Given that outside of the Arctic, LIS iceberg discharge probably did not increase during the Bølling, much of the LIS MWP-1A contribution likely occurred through surface ablation. Here we test the response of LIS surface mass-balance to Bølling warming by forcing a LIS energy–mass balance model with climate from an atmosphere–ocean general circulation model. Our modeling approach neglects changes in LIS mass from dynamics and iceberg calving, allowing us to isolate the surface mass balance response. Model results suggest that LIS surface ablation can explain much of the sea-level rise just prior to MWP-1A. LIS surface mass-balance becomes more negative in response to the Bølling warming, contributing an additional 2.9 ± 1.0 m of sea-level rise in 500 yr in addition to the background contribution of 4.0 ± 0.8 m. The modeled LIS MWP-1A contribution is less than previous assumptions but agrees with geochemical runoff and LIS area-volume estimates. The fraction of MWP-1A attributable to other ice sheets, particularly Antarctica, depends on the total sea-level rise that occurred during this MWP.

1. Introduction

During the last deglaciation ~20–6 ka, sea level rose 125–130 m at an average rate of ~1 cm yr^{-1} (Bard et al., 1990; Fairbanks, 1989). The rate of sea-level rise was not constant with several intervals of more rapid rise, the most notable of which is Meltwater Pulse (MWP) 1A (Fairbanks, 1989; Hanebuth et al., 2000; Peltier and Fairbanks, 2006). During MWP-1A, sea level rose 10–20 m in <500 yrs, indicating rapid mass loss from one or more ice sheets to the global oceans (Fig. 1C). The timing of MWP-1A is roughly coincident with the abrupt warming of the North Atlantic region into the Bølling ~14.6 ka (Fig. 1A). The precise relationship is debatable, however, with the onset of MWP-1A ranging from ~14.6 to 14.3 ka and termination between ~14.6 and 13.8 ka (Fig. 1C) (Bard et al., 1990; Edwards et al., 1993; Hanebuth et al., 2000; Peltier and Fairbanks, 2006; Stanford et al., 2006; Weaver et al., 2003). Thus MWP-1A could be coincident with or lag the onset of the Bølling warm period, with implications for the sources and climatic impacts of this MWP (Stanford et al., 2006; Tarasov and Peltier, 2005; Weaver et al., 2003).

The Laurentide Ice Sheet (LIS) was originally assumed to be the dominant source of MWP-1A (e.g., Fairbanks, 1989; Peltier, 1994) with subsequent work suggesting additional contributions from the Scandinavian, Barents–Kara and Cordilleran Ice Sheets (Peltier, 2004; Tarasov and Peltier, 2005). A large LIS contribution could be explained as a response to the abrupt Bølling warming with the majority of the meltwater delivered to the ocean through increased surface ablation of its southern margin (Peltier, 2004; Tarasov and Peltier, 2005). In as much as increased deposition of iceberg rafted debris (IRD) sourced from the LIS reflects increased iceberg calving, IRD records suggest that eastern LIS iceberg discharge did not significantly increase during the Bølling (Fig. 1B) (e.g., Andrews and Tedesco, 1992; Bond et al., 1999; Hemming, 2004; Keigwin and Jones, 1995). IRD deposition in the Arctic Ocean, however, increased and may record the onset of northern LIS retreat and greater iceberg calving during the Bølling (Darby et al., 2002; Dyke, 2004; England et al., 2009). Here we investigate the LIS surface mass-balance response-alone to Bølling warming by forcing an energy–mass balance model (EMBM) with climate fields from an atmosphere–ocean general circulation model

* Corresponding author at: Department of Geoscience, University of Wisconsin, Madison, WI 53706, USA.
E-mail address: acarlson@geology.wisc.edu (A.E. Carlson).

0012-821X/$ – see front matter © 2011 Elsevier B.V. All rights reserved.
doi:10.1016/j.epsl.2011.07.008

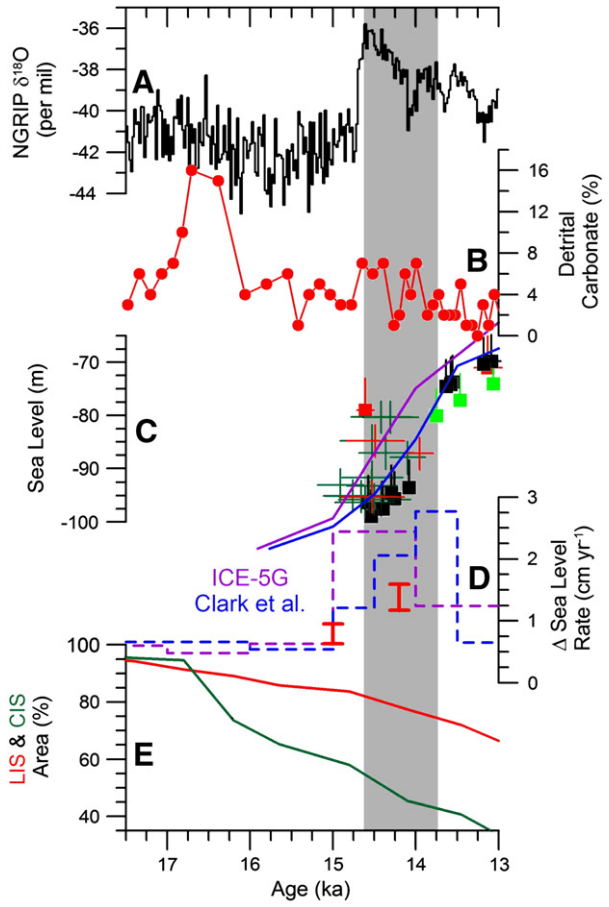

Fig. 1. Climate and sea level. (A) Greenland $\delta^{18}O$ (Svensson et al., 2008). (B) North Atlantic % detrital carbonate from core V23-81 (Bond et al., 1999). (C) Eustatic and relative sea level. Purple line is ICE-5G eustatic (Peltier, 2004); blue line is eustatic sea level from Clark et al. (2009). Squares are coral sea-level data (red from New Guinea, light green from Tahiti, black from Barbados) (Bard et al., 1996; Edwards et al., 1993; Peltier and Fairbanks, 2006). Crosses are mangrove sea-level data from Sunda Shelf (red are in situ, dark green are not in situ) (Hanebuth et al., 2000). Depth and age range indicated for relative sea-level data. (D) Rate of eustatic sea-level rise (Clark et al., 2009; Peltier, 2004) and EMBM-modeled LIS contributions (red vertical bars). (E) Percent of the LIS (red) and CIS (dark green) remaining relative to Last Glacial Maximum extent (Dyke, 2004). Vertical gray bar denotes the range in MWP-1A timing with its duration being <500 yr (Bard et al., 1990; Edwards et al., 1993; Hanebuth et al., 2000; Stanford et al., 2006; Weaver et al., 2003). (For interpretation of the references to color in this figure legend, the reader is referred to the web version of this article.)

(AOGCM) that simulated the abrupt onset of the Bølling following the Oldest Dryas cold period ~18.5–14.6 ka (Liu et al., 2009).

2. Modeling LIS surface mass-balance

We use the EMBM of Anslow et al. (2008) to simulate the surface mass-balance of the LIS near the end of the Oldest Dryas (~15 ka) and during the Bølling (~14.2 ka). The EMBM accounts for spatial and temporal changes in a melting snow or ice surface including surface roughness and geometry with respect to incoming shortwave radiation. Meltwater refreezing is simulated following Huybrechts and deWolde (1999) (Carlson et al., 2009). Snow and ice albedos are assumed 0.8 and 0.5, respectively, based on observations of the Greenland Ice Sheet (e.g., Greuell, 2000), which is the only potential modern analog for the LIS. We use a range of surface roughness lengths for snow (0.001–0.0001 m) and ice (0.01–0.05 m) also based on Greenland Ice Sheet measurements (e.g., Duynkerke and van den Broeke, 1994; Grainger and Lister, 1966; Greuell and Konzelmann, 1994; Smeets and van den Broeke, 2008). This model only accounts for changes in surface ablation, and neglects dynamic feedbacks such as ice surface lowering and mass loss from calving to the ocean.

The EMBM is forced with air temperature, wind speed and direction, humidity, surface shortwave radiation, downward longwave radiation, and precipitation taken from the National Center for Atmospheric Research Community Climate System Model 3 (NCAR CCSM3; Collins et al., 2006) transient simulation described in Liu et al. (2009). CCSM3 is a fully coupled AOGCM with dynamic-vegetation and sea-ice modules. The atmosphere has 26 levels and ~3.75° horizontal resolution. The ocean has 25 levels, longitudinal resolution of 3.6° and varying latitudinal resolution that increases to ~0.9° at the equator, with higher resolution also in the North Atlantic. CCSM3 was forced with transient changes in the orbit of the Earth, greenhouse gasses, reconstructed ice sheets (ICE-5G; Peltier, 2004) and meltwater flux to the oceans (Peltier, 2004) from 22 to 14.5 ka. The meltwater flux deviated from that of Peltier (2004) after 14.5 ka, and MWP-1A was not applied in these simulations. If such a flux had been added to the North Atlantic, the model would have failed to produce the Bølling warming (Liu et al., 2009).

The AOGCM successfully simulated cooling during the Oldest Dryas in response to Northern Hemisphere ice-sheet retreat and the magnitude of abrupt warming into the Bølling from a subsequent reduction of meltwater discharge to the North Atlantic (Liu et al., 2009). In particular, this AOGCM reproduced the Bølling warming of 9 ± 3 °C observed over Greenland (Severinghaus and Brook, 1999) and in the North Atlantic of ~6 °C (Bard et al., 2000), providing us confidence in using it as a reasonable climate forcing. We note, however, that AOGCMs can have biases in their absolute simulated climate. Of importance for our study is the sensitivity of CCSM3 to the reduction in meltwater discharge during the Oldest Dryas-Bølling transition, because CO_2 did not significantly change 14.5–14.0 ka. CCSM3 simulates a 25–40% reduction in Atlantic meridional overturning strength in response to 0.1 Sverdrups (Sv; 10^6 m^3 s^{-1}) of freshwater forcing to the North Atlantic, the range depending on the location and duration of the freshwater forcing, with a subsequent recovery upon removal of the freshwater forcing (Otto-Bliesner and Brady, 2010). This compares well with the average reduction of ~30% (range 5–60%) for a 0.1 Sv freshwater forcing for 100 yr followed by recovery as determined from a suite of climate models (Stouffer et al., 2006), suggesting CCSM3 has a reasonable sensitivity to freshwater discharge. Nevertheless, we have greater confidence in the simulated change in the LIS mass balance from Bølling warming, upon which we focus discussion.

We use 50-year averages from the transient DGL-A simulation at 15.05–15.00 ka and 14.25–14.20 ka. Of the two CCSM3 simulations performed with different meltwater forcing schemes (DGL-A and DGL-B), DGL-A showed the greatest agreement with proxy climate reconstructions (Liu et al., 2009) and thus was selected for our study. This simulation also had the greatest abrupt Bølling warming and thus the greatest difference in climate between ~15.0 and 14.2 ka. As mentioned above, MWP-1A was not applied to the global oceans in this simulation, which if applied to the North Atlantic would have significantly reduced Atlantic meridional overturning circulation in the model (Liu et al., 2009). By excluding this freshwater forcing, we allow for the maximum overturning circulation recovery at the time of the Bølling warming and thus maximum warming. Given this obvious extreme forcing on the EMBM, our results should be viewed as maximum estimates of the LIS surface mass-balance response to Bølling warming as simulated by this AOGCM.

We downscale vertically and horizontally the CCSM3 simulation following standard methods to a 50×50 km LIS topography taken from ICE-5G for 15 ka (pre-Bølling) and 14.5 ka (Bølling) (Peltier, 2004) using LIS-appropriate atmospheric lapse rates (-5 °C km^{-1} for temperature and 0.1 km^{-1} for precipitation) for elevation-sensitive variables (Abe-Ouchi et al., 2007; Carlson et al., 2009; Marshall et al., 2002; Pollard et al., 2000). We note that changes in the ICE-5G LIS topography are minimal between 15 and 14.5 ka (Peltier, 2004) and

Please cite this article as: Carlson, A.E., et al., Modeling the surface mass-balance response of the Laurentide Ice Sheet to Bølling warming and its contribution to Meltwater Pulse 1A, Earth Planet. Sci. Lett. (2011), doi:10.1016/j.epsl.2011.07.008

thus changes in LIS surface mass balance are attributable to Bølling warming rather than geometric factors. We also assess the effects of a lower, post-MWP-1A LIS by using the ICE-5G 14 ka LIS topography, which has a lower inner LIS dome and retracted ice margins relative to 14.5 ka (Peltier, 2004). For simplicity, we convert the surface mass-balance values to equivalent rates of sea-level rise.

3. LIS surface mass-balance response to Bølling warming

During the latter part of the Oldest Dryas, the EMBM simulates a net LIS surface mass-balance that equates to 0.79 ± 0.16 cm yr^{-1} of equivalent sea-level rise (uncertainty reflects the total range of results from varied snow and ice roughness length) (Figs. 1D and 2A; Table 1). Ablation is focused along the southern and northwestern LIS margins at rates up to ~4 m yr^{-1} (Fig. 2C). Net accumulation occurs in the northern 1/3 of the ice sheet and along the southern and southeastern margin (Fig. 2B). Much of the interior LIS receives <0.6 m yr^{-1} of precipitation, which is more than offset by sublimation (Fig. 2C). The existence of a large Keewatin Dome in the ICE-5G reconstruction likely caused this very dry interior (Otto-Bliesner et al., 2006), the validity of which should be tested with alternative LIS configurations but is beyond the scope of this study.

The warming into the Bølling decreases modeled LIS total surface mass-balance that equates to 1.38 ± 0.21 cm yr^{-1} of equivalent sea-level rise (Figs. 1D and 2D; Table 1). Much of this increased mass loss comes from greater surface ablation along the southern and northwest LIS margins where ablation increases by 4–6 m yr^{-1} (Figs. 2F and 3C). The surface mass balance of the LIS interior remains largely unaffected by Bølling warming (Fig. 3B), but there is a slight increase in precipitation in the northwest (Fig. 2E). Precipitation also increases over the southeastern LIS by ≤0.4 m yr^{-1} causing a local net mass balance increase of ≤1.0 m yr^{-1} due to increased precipitation and the attendant increase in albedo.

We assess the effects that topographic lowering and ice-margin retreat would have on LIS surface mass-balance by using the post MWP-1A LIS topography that has an assumed LIS MWP-1A contribution of 16.5 m of equivalent sea-level rise (Fig. 2G) (Peltier, 2004). The LIS surface mass-balance is 0.73 ± 0.25 cm yr^{-1} of equivalent sea-level rise (Table 1). Retreat of the low elevation southern and northwestern LIS margins and the attendant loss of the extensive ablation zone cause much of this increase in mass balance (Fig. 2I).

Just prior to the Bølling, the EMBM simulates that LIS surface mass-balance of 0.79 ± 0.16 cm yr^{-1} of equivalent sea-level rise would raise sea level 4.0 ± 0.8 m in 500 yr (Table 1). The LIS simulated surface mass-balance of 1.38 ± 0.21 cm yr^{-1} of equivalent sea-level rise during the Bølling equates to 6.9 ± 1.1 m of equivalent sea-level rise in 500 yr. The difference between these two simulations of 0.59 ± 0.19 cm yr^{-1} of equivalent sea-level rise results in 2.9 ± 1.0 m of sea-level rise in 500 yr and corresponds to the LIS surface mass-balance response attributable to Bølling warming, neglecting the effects of dynamics and calving on the total LIS mass budget. As noted in Section 2, we place greater confidence in this modeled change in LIS surface mass-balance between the Oldest Dryas and the Bølling.

4. Comparison of LIS surface mass-balance with deglacial records

The EMBM simulates that the southern and northwestern LIS margins were the most sensitive to Bølling warming and the locations

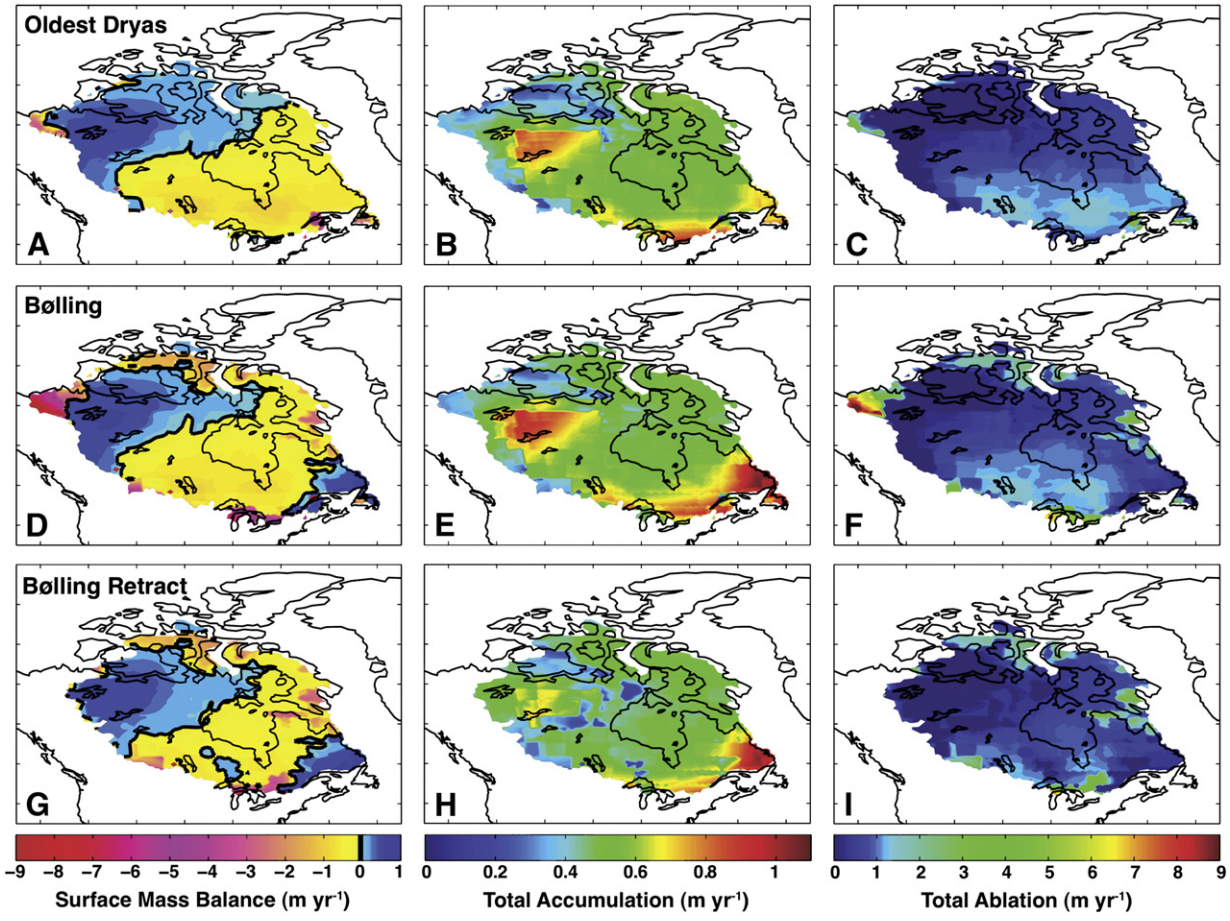

Fig. 2. LIS surface mass-balance (left), accumulation (center), and ablation (right) for the Oldest Dryas (A–C), Bølling (D–F), and Bølling with retracted LIS topography (G–I). These figures show results for simulations that produce the mean of range in possible surface mass-balances.

Please cite this article as: Carlson, A.E., et al., Modeling the surface mass-balance response of the Laurentide Ice Sheet to Bølling warming and its contribution to Meltwater Pulse 1A, Earth Planet. Sci. Lett. (2011), doi:10.1016/j.epsl.2011.07.008

Table 1
Surface mass-balance model results.

Time period	Surface mass-balance (myr^{-1})	Surface ablation (myr^{-1})	Sea-level rise ($cm\ yr^{-1}$)	500 yr sea-level rise (m)
Oldest Dryas (15.0 ka)	-0.28 ± 0.06	-0.87 ± 0.06	0.79 ± 0.16	4.0 ± 0.8
Bølling (14.2 ka)	-0.49 ± 0.07	-1.10 ± 0.07	1.38 ± 0.21	6.9 ± 1.1
Retracted Bølling (14.2 ka)	-0.30 ± 0.10	-0.83 ± 0.10	0.73 ± 0.25	3.7 ± 1.3

of significant mass loss (Fig. 3). Upon removal of these low-elevation regions, the LIS surface mass-balance increases to approximately pre-Bølling levels (Fig. 2; Table 1). Although not directly comparable because our model lacks dynamics, we qualitatively assess the model performance with LIS deglacial records. Supporting our model simulations, radiocarbon dates indicate that following the Port Huron readvance 15.0–14.7 ka, the southern LIS margin retreated during the Bølling culminating in the Two Creeks interstade ~13.8 ka (Hansel and Johnson, 1992; Hansel and Mickelson, 1988; Licciardi et al., 1999). The chronology for the northwest LIS margin similarly indicates ice retreat during the Bølling also in agreement with our model simulations (Dyke, 2004; England et al., 2009). The increase in precipitation over the southeast LIS may have offset the effects of Bølling warming in this region (Fig. 3A), explaining why ice remained on the coasts of Labrador and Quebec during the Bølling with even the potential for a small ice readvance (Dyke, 2004). By scaling ice area to volume, the LIS area deglaciated between ~14.8 and 14.1 ka, corresponding to a LIS contribution to sea level rise of 4.3 ± 0.5 m (Carlson, 2009), which is slightly lower than these EMBM results (see Section 3) (the uncertainty in the estimate reflects the different ice-sheet and -cap relationships between basal shear, ice temperature and the ice surface profile used to derive the empirical scaling; Paterson, 1994). This area-volume scaling assumes an ice sheet in equilibrium (Paterson, 1994), however, which was not the case during the Bølling, and thus could underestimate the amount of LIS mass loss.

Marine records also indicate northwestern and southern LIS retreat during the Bølling, with decreased planktonic $\delta^{18}O$ and increased IRD in the Arctic Ocean and decreased seawater $\delta^{18}O$ in the Gulf of Mexico potentially reflecting increased LIS mass loss (Darby et al., 2002; Flower et al., 2004; Hall and Chan, 2004; Poore et al., 1999). Off of the Gulf of St. Lawrence, planktonic $\delta^{18}O$ also decreased (Keigwin et al., 2005). However, this decrease was caused by Bølling warming and seawater $\delta^{18}O$ increased off of the Gulf of St. Lawrence, suggesting a reduction in LIS ablation and/or that meltwater was not routed toward the Northwest Atlantic (Obbink et al., 2010), in agreement with IRD records (Keigwin and Jones, 1995) and our surface mass-balance simulations (Fig. 3). A runoff-ocean mixing model simulated that these abrupt decreases in $\delta^{18}O$ reflect increased LIS ablation equivalent to ≤ 5.3 m of sea-level rise in 500 yr (Carlson, 2009). For comparison, the EMBM simulated Bølling increase in surface ablation (Fig. 2F; Table 1) is equivalent to 3.5 ± 1.2 m of sea-level rise in 500 yr, in agreement with the runoff $\delta^{18}O$ estimate.

5. Implications for the sources of MWP-1A

Sea-level models suggest pre-MWP-1A rates of global mean sea-level rise between ~0.6 (ICE-5G) and 1.2 (Clark et al.) $cm\ yr^{-1}$ (Fig. 1D) (Clark et al., 2009; Peltier, 2004). Our simulated Oldest Dryas LIS surface mass-balance of $0.79 \pm 0.16\ cm\ yr^{-1}$ of equivalent sea-level rise can explain much of the pre-MWP-1A rate of sea-level rise. The same eustatic models suggest maximum MWP-1A rates of sea-level rise between ~2.4 (ICE-5G) and 2.8 (Clark et al.) $cm\ yr^{-1}$. MWP-1A therefore represents an increase in the rate of sea-level rise by 1.6–1.8 $cm\ yr^{-1}$, of which the decrease in LIS surface mass-balance by $0.59 \pm 0.19\ cm\ yr^{-1}$ of equivalent sea-level rise can account for $37 \pm 13\%$.

An additional LIS sea-level rise contribution may have come through increased iceberg calving, which is neglected in our model. Detrital carbonate and IRD records from the North Atlantic suggest, however, little change in LIS iceberg discharge from the late Oldest Dryas to the Bølling (Fig. 1B) (e.g., Andrews and Tedesco, 1992; Bond et al., 1999; Hemming, 2004; Keigwin and Jones, 1995). Increased calving would therefore probably not explain any significantly large acceleration in mass loss during the Bølling from the marine-terminating portion of the eastern LIS. As mentioned previously, IRD records from the Arctic Ocean imply increased calving of the northwestern LIS marine margin during the Bølling (Darby et al., 2002). Although our modeling approach cannot assess the magnitude of this additional mass loss to the Arctic Ocean, previous estimates based on the decrease in planktonic $\delta^{18}O$ (Poore et al., 1999) suggest that ~0.5 m of sea-level equivalent volume was discharged to the Arctic Ocean during MWP-1A (Carlson, 2009). The effect of meltwater penetrating to the ice bed and facilitating basal sliding (e.g., Joughin et al., 2008; Zwally et al., 2002) is also neglected in our model, which could thin the LIS and increase ablation, but the impacts of this feedback remain uncertain and may be relatively small (e.g., Carlson et al., 2007; Sundal et al., 2011).

The ICE-5G model we used in the AOGCM and EMBM has an assumed LIS MWP-1A contribution of 16.5 m of equivalent sea-level rise at a rate of 1.65 $cm\ yr^{-1}$ for 1000 yr, which is an increase in the rate of LIS mass loss above the preceding Oldest Dryas of 1.45 $cm\ yr^{-1}$

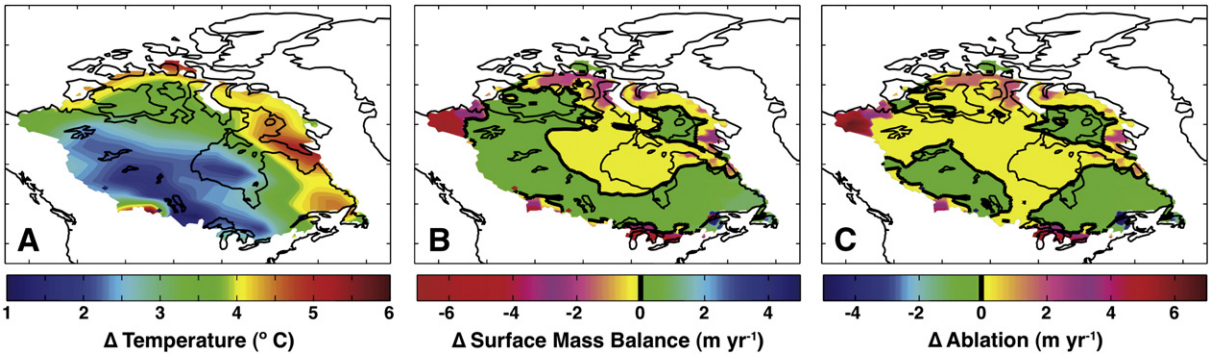

Fig. 3. Change in late boreal summer (August 1) surface air temperatures simulated by CCSM3 between the Oldest Dryas and Bølling (A), and resulting difference in LIS surface mass balance (B) and ablation (C).

Please cite this article as: Carlson, A.E., et al., Modeling the surface mass-balance response of the Laurentide Ice Sheet to Bølling warming and its contribution to Meltwater Pulse 1A, Earth Planet. Sci. Lett. (2011), doi:10.1016/j.epsl.2011.07.008

(Peltier, 2004). The majority of this ice mass is discharged through the southern LIS margin (Peltier, 2004), where the ice must have been delivered to the ocean via surface ablation. Our AOGCM-EMBM approach simulates, however, that Bølling warming would only cause an increase in net LIS surface ablation equivalent to 0.59 ± 0.19 cm yr^{-1} of additional sea-level rise, which is 28–54% of the rate for the 1000-year long LIS MWP-1A contribution in ICE-5G. Given that the Bølling warming and MWP-1A both lasted for ~500 yr (Fig. 1), we suggest that the ICE-5G assumed LIS-contribution to MWP-1A may be too large.

A dynamic LIS model simulated 7.8 ± 0.2 to 9.9 ± 0.3 m of equivalent sea-level rise from the LIS during MWP-1A that includes Cordilleran Ice Sheet contributions (Tarasov and Peltier, 2005; 2006). Peak increases in the rate of sea-level rise range from 2.52 ± 0.13 to 2.72 ± 0.15 cm yr^{-1}, with 500-yr average increases between 1.06 ± 0.03 and 1.41 ± 0.11 cm yr^{-1}, which is higher than our Bølling increase in the rate sea-level rise from the LIS alone of 0.59 ± 0.19 cm yr^{-1}. These two different approaches still do not agree if the Cordilleran component is removed by assuming ~90% of the MWP-1A contribution is from the LIS (~0.95–1.27 cm yr^{-1}) (Dyke, 2004; Tarasov and Peltier, 2006). This LIS-Cordilleran dynamic model relied on Summit Greenland δ^{18}O records to generate the temperature and precipitation forcing. The larger MWP-1A contribution in this LIS-model may result from this simplified climate forcing that may overestimate the Bølling warming in North America, given its location up-wind of the climate forcing record (Tarasov and Peltier, 2004) and potential issues with directly scaling ice-core δ^{18}O to temperature (LeGrande and Schmidt, 2009). Furthermore, MWP-1A is a forced event in their model induced in the same manner as Heinrich Events through an increase in till viscosity several thousand years prior to the event and a decrease at the time of MWP-1A, which also explains the larger MWP-1A contribution from this ice sheet model (Stokes and Tarasov, 2009). Because of the very different climate changes surrounding Heinrich Events relative to MWP-1A and the Bølling (e.g., Clark et al., 2002b; 2007; Hemming, 2004; Shakun and Carlson, 2010; Weaver et al., 2003), we question the applicability of this approach for simulating MWP-1A.

Multiple lines of evidence therefore point towards 5–7 m of sea-level rise coming from the LIS around the time of MWP-1A with a more abrupt sea-level rise contribution attributable to Bølling warming of <5 m. The geologic record suggests a substantially smaller contribution to sea-level rise from the Scandinavian Ice Sheet during MWP-1A (Goehring et al., 2008; Karpuz and Jansen, 1992; Lehman et al., 1991; Rinterknecht et al., 2006), whereas the Barents–Kara Ice Sheet had already collapsed prior to MWP-1A (Jones and Keigwin, 1988; Svendsen et al., 2004). Although the Cordilleran Ice Sheet lost ~13% of its area around the time of MWP-1A (Fig. 1E), its small size rules out a major contribution to MWP-1A (e.g., 1.2 ± 0.2 m of equivalent sea-level rise based on area-volume scaling, which is likely an overestimate given the underlying mountainous terrain; Dyke, 2004; Paterson, 1994).

The Antarctica contribution to MWP-1A largely depends on the eustatic rise in sea level during MWP-1A. If the actual amount of sea-level rise was close to 10 m eustatic, the majority of this MWP could be explained by Northern Hemisphere sources. If, however, MWP-1A was closer to 15–20 m of sea-level rise, a significant fraction must have been sourced from the Antarctic Ice Sheets (Clark et al., 1996), which is supported by some geophysical Earth model simulations and sea-level fingerprinting (Bassett et al., 2005; Clark et al., 2002a). Peltier (2005) argued that fingerprinting could not differentiate the sources of MWP-1A but also utilized an undocumented deglaciation history for the Northern Hemisphere (Peltier, 1994) that is inconsistent with the above discussed geologic record for the Cordilleran and Barents–Kara Ice Sheets. Moreover, his predictions for post MWP-1A sea level at far-field sites show strong misfits with observations, which largely disappears when a significant Antarctic MWP-1A contribution is included (Bassett et al., 2005). Although still debated in terms of the magnitude of retreat/thinning and attendant sea-level rise contributions, there is growing evidence that the onset of deglaciation in the Ross Sea, Weddell Sea, Pine Island Bay, and Mac. Robertson Land sectors of the Antarctic Ice Sheets occurred 14–15 ka (Bentley et al., 2010; Clark, 2011; Clark et al., 2009; Hall and Denton, 2000; Johnson et al., 2008; Mackintosh et al., 2011; Price et al., 2007; Todd et al., 2010) and that marine-terminating ice on the Antarctic Peninsula and in the Amundsen Sea retreated rapidly during MWP-1A (Heroy and Anderson, 2007; Kilfeather et al., 2011; Smith et al., 2011), supporting the hypothesis (Clark et al., 1996; 2002a; Weaver et al., 2003) that the Antarctic Ice Sheets also contributed to MWP-1A.

Acknowledgments

The authors wish to thank Lev Tarasov for kindly sharing his model simulation results and three reviewers for their comments and suggestions. This research was supported by National Science Foundation AGS grants 1002531 (Z.L., B.O.-B., A.E.C.) and 0753660 (A.E.C.), and by the National Science Foundation Paleoclimate Program to P.U.C.

References

Abe-Ouchi, A., Segawa, T., Saito, F., 2007. Climatic conditions for modelling the Northern Hemisphere ice sheets throughout the ice age cycle. Clim. Past 3, 423–438.
Andrews, J.T., Tedesco, K., 1992. Detrital carbonate-rich sediments, northwestern Labrador Sea: implications for ice-sheet dynamics and iceberg rafting (Heinrich) events in the North Atlantic. Geology 20, 1087–1090.
Anslow, F.S., Hostetler, S., Bidlake, W.R., Clark, P.U., 2008. Distributed energy balance modeling of South Cascade Glacier, Washington and assessment of model uncertainty. J. Geophys. Res. 113, F02019. doi:10.1029/2007JF000850.
Bard, E., Hamelin, B., Fairbanks, R.G., Zindler, A., 1990. Calibration of the ^{14}C timescale over the past 30,000 years using mass spectrometric U–Th ages from Barbados corals. Nature 345, 405–410.
Bard, E., Hamelin, B., Arnold, M., Montaggioni, L., Cabioch, G., Faure, G., Rougerie, F., 1996. Deglacial sea-level record from Tahiti corals and the timing of global meltwater discharge. Nature 382, 241–244.
Bard, E., Rostek, F., Turon, J.-L., Gendreau, S., 2000. Hydrological impact of Heinrich events in the subtropical Northeast Atlantic. Science 289, 1321–1324.
Bassett, S.E., Milne, G.A., Mitrovica, J.X., Clark, P.U., 2005. Ice sheet and solid Earth influences on far-field sea-level histories. Science 309, 925–928.
Bentley, M.J., Fogwill, C.J., Le Brocq, A.M., Hubbard, A.L., Sugden, D.E., Dunai, T.J., Freeman, S.P.H.T., 2010. Deglacial history of the West Antarctic Ice Sheet in the Weddell Sea embayment: constraints on past ice volume change. Geology 38, 411–414.
Bond, G.C., Showers, E., Elliot, M., Evans, M., Lotti, R., Hajdas, I., Bonani, G., Johnsen, S., 1999. The North Atlantic's 1–2 kyr climate rhythm: relation to Heinrich events, Dansgaard/Oeschger cycles and the little ice age. In: Clark, P.U., Webb, R.S., Keigwin, L.D. (Eds.), Mechanisms of global climate change at millennial time scales: AGU Geophys. Monogr., 112, pp. 35–58.
Carlson, A.E., 2009. Geochemical constraints on the Laurentide Ice Sheet contribution to Meltwater Pulse 1A. Quat. Sci. Rev. 28, 1625–1630.
Carlson, A.E., Jenson, J.W., Clark, P.U., 2007. Modeling the subglacial hydrology of the James Lobe of the Laurentide Ice Sheet. Quat. Sci. Rev. 26, 1384–1397.
Carlson, A.E., Anslow, F.S., Obbink, E.A., LeGrande, A.N., Ullman, D.J., Licciardi, J.M., 2009. Surface-melt driven Laurentide Ice Sheet retreat during the early Holocene. Geophys. Res. Lett. 36, L24502. doi:10.1029/2009GL040948.
Clark, P.U., 2011. Deglacial history of the West Antarctic Ice Sheet in the Weddell Sea embayment: constraints on past ice volume change: COMMENT. Geology 39. doi:10.1130/G31533C.1.
Clark, P.U., Alley, R.B., Keigwin, L.D., Licciardi, J.M., Johnsen, S., Wang, H., 1996. Origin of the first global meltwater pulse following the last glacial maximum. Paleoceanography 11, 563–577.
Clark, P.U., Mitrovica, J.X., Milne, G.A., Tamisiea, M.E., 2002a. Sea-level fingerprinting as a direct test for the source of global Meltwater Pulse IA. Science 295, 2438–2441.
Clark, P.U., Pisias, N.G., Stocker, T.F., Weaver, A.J., 2002b. The role of the thermohaline circulation in abrupt climate change. Nature 415, 863–869.
Clark, P.U., Hostetler, S.W., Pisias, N.G., Schmittner, A., Meissner, K.J., 2007. Mechanisms for an ~7-kyr climate and sea-level oscillation during marine isotope state 3. In: Schmittner, A., Chiang, J., Hemming, S. (Eds.), Ocean Circulation: Mechanisms and Impacts: AGU Geophys. Monogr., 173, pp. 209–246.
Clark, P.U., Dyke, A.S., Shakun, J.D., Carlson, A.E., Clark, J., Wohlfarth, B., Mitrovica, J.X., Hostetler, S.W., McCabe, A.M., 2009. The last glacial maximum. Science 325, 710–714.
Collins, W.D., Bitz, C.M., Blackmon, M.L., Bonan, G.B., Bretherton, C.S., Carton, J.A., Chang, P., Doney, S.C., Hack, J.J., Henderson, T.B., Kiehl, J.T., Large, W.G., McKenna, D.S., Santer,

Please cite this article as: Carlson, A.E., et al., Modeling the surface mass-balance response of the Laurentide Ice Sheet to Bølling warming and its contribution to Meltwater Pulse 1A, Earth Planet. Sci. Lett. (2011), doi:10.1016/j.epsl.2011.07.008

B.D., Smith, R.D., 2006. The Community Climate System Model version 3 (CCSM3). J. Climate 19, 2122–2143.
Darby, D.A., Bischof, J.F., Spielhagen, R.F., Marshall, S.A., Herman, S.W., 2002. Arctic ice export events and their potential impact on global climate during the late Pleistocene. Paleoceanography 17. doi:10.1029/2001PA000639.
Duynkerke, P.G., van den Broeke, M.R., 1994. Surface energy balance and katabatic flow over glacier and tundra during GIMEX-91. Global Planet. Change 9, 17–28.
Dyke, A.S., 2004. An outline of North American Deglaciation with emphasis on central and northern Canada. In: Ehlers, J., Gibbard, P.L. (Eds.), Quaternary Glaciations: Extent and Chronology. Elsevier, Amsterdam, pp. 373–424.
Edwards, R.L., Beck, J.W., Burr, G.S., Donahue, D.J., Chappell, J.M.A., Bloom, A.L., Druffel, E.R.M., Taylor, F.W., 1993. A large drop in atmospheric $^{14}C/^{12}C$ and reduced melting in the Younger Dryas, documented with ^{230}Th ages of corals. Science 260, 962–968.
England, J.H., Furze, M.F.A., Doupé, J.P., 2009. Revision of the NW Laurentide Ice Sheet: implications for paleoclimate, the northeast extremity of Beringia, and Arctic Ocean sedimentation. Quat. Sci. Rev. 28, 1573–1596.
Fairbanks, R.G., 1989. A 17,000-year glacio-eustatic sea level record: influence of glacial melting rates on the Younger Dryas event and deep-ocean circulation. Nature 342, 637–642.
Flower, B.P., Hastings, D.W., Hill, H.W., Quinn, T.M., 2004. Phasing of deglacial warming and Laurentide Ice Sheet meltwater in the Gulf of Mexico. Geology 32, 597–600.
Goehring, B.M., Brook, E.J., Linge, H., Raisbeck, G.M., Yiou, F., 2008. Beryllium-10 exposure ages of erratic boulders in southern Norway and implications for the history of the Fennoscandian Ice Sheet. Quat. Sci. Rev. 27, 320–336.
Grainger, M.E., Lister, H., 1966. Wind speed, stability and eddy viscosity over melting ice surfaces. J. Glaciol. 6, 101–127.
Greuell, W., 2000. Melt-water accumulation on the surface of the Greenland Ice sheet: effect of albedo and mass balance. Geogr. Ann. 82, 489–498.
Greuell, W., Konzelmann, T., 1994. Numerical modelling of the energy balance and the englacial temperature of the Greenland Ice Sheet. Calculations for the ETH-Camp location (West Greenland, 115 m a.s.l.). Global Planet. Change 9, 91–114.
Hall, J.M., Chan, L.-H., 2004. Ba/Ca in *Neogloboquadrina pachyderma* as an indicator of deglacial meltwater discharge into the western Arctic Ocean. Paleoceanography 19. doi:10.1029/2003PA000910.
Hall, B.L., Denton, G.H., 2000. Radiocarbon chronology of Ross Sea drift, Eastern Taylor Valley, Antarctica: evidence for a grounded ice sheet in the Ross Sea at the Last Glacial Maximum. Geogr. Ann. 82, 305–336.
Hanebuth, T., Stattegger, K., Grootes, P.M., 2000. Rapid flooding of the Sunda Shelf: a Late-Glacial sea-level record. Science 288, 1033–1035.
Hansel, A.K., Johnson, W.H., 1992. Fluctuations of the Lake Michigan lobe during the late Wisconsin subepisode. Sver. Geol. Unders. 81, 133–144.
Hansel, A.K., Mickelson, D.M., 1988. A reevaluation of the timing and causes of high lake phases in the Lake Michigan basin. Quat. Res. 29, 113–128.
Hemming, S.R., 2004. Heinrich events: massive Late Pleistocene detritus layers of the North Atlantic and their global imprint. Rev. Geophys. 42. doi:10.1029/2003RG000128.
Heroy, D.C., Anderson, J.B., 2007. Radiocarbon constraints on Antarctic Peninsula Ice Sheet retreat following the Last Glacial Maximum (LGM). Quat. Sci. Rev. 26, 3286–3297.
Huybrechts, P., deWolde, J., 1999. The dynamic response of the Greenland and Antarctic ice sheets to multiple-century climate warming. J. Climate 12, 2169–2188.
Johnson, J.S., Bentley, M.J., Gohl, K., 2008. First exposure ages from the Amundsen Sea Embayment, West Antarctica: The Late Quaternary context for recent thinning of Pine Island, Smith, and Pope Glaciers. Geology 36, 223–226.
Jones, G.A., Keigwin, L.D., 1988. Evidence from Fram Strait (78° N) for early deglaciation. Nature 336, 56–59.
Joughin, I., Das, S.B., King, M.A., Smith, B.E., Howat, I.M., Moon, T., 2008. Seasonal speedup along the western flank of the Greenland Ice Sheet. Science 320, 781–783.
Karpuz, N.A., Jansen, E., 1992. A high-resolution diatom record of the last deglaciation from the southeast Norwegian Sea: documentation of rapid climatic changes. Paleoceanography 7, 499–520.
Keigwin, L.D., Jones, G.A., 1995. The marine record of deglaciation from the continental margin off Nova Scotia. Paleoceanography 10, 973–985.
Keigwin, L.D., Sachs, J.P., Rosenthal, Y., Boyle, E.A., 2005. The 8200 year B.P. event in the slope water system, western subpolar North Atlantic. Paleoceanography 20. doi:10.1029/2004PA001074.
Kilfeather, A.A., Ó Cofaigh, C., Lloyd, J.M., Dowdeswell, J.A., Xu, S., Moreton, S.G., 2011. Ice-stream retreat and ice-shelf history in Marguerite Trough, Antarctic Peninsula: sedimentological and foraminiferal signatures. Geol. Soc. Am. Bull. 123, 997–1015.
LeGrande, A.N., Schmidt, G.A., 2009. Sources of Holocene variability of oxygen isotopes in paleoclimate archives. Clim. Past 5, 441–455.
Lehman, S.J., Jones, G.A., Keigwin, L.D., Andersen, E.S., Butenko, G., 1991. Initiation of Fennoscandian ice sheet retreat during the last deglaciation. Nature 349, 513–516.
Licciardi, J.M., Teller, J.T., Clark, P.U., 1999. Freshwater routing by the Laurentide ice sheet during the last deglaciation. In: Clark, P.U., Webb, R.S., Keigwin, L.D. (Eds.), Mechanisms of global climate change at millennial time scales: AGU Geophys. Monogr., 112, pp. 177–201.
Liu, Z., Otto-Bliesner, B.L., He, F., Brady, C.E., Tomas, R., Clark, P.U., Carlson, A.E., Lynch-Stieglitz, J., Curry, W., Brook, E., Erickson, D., Jacob, R., Kutzbach, J., Cheng, J., 2009. Transient climate simulation of last deglaciation towards Bølling/Allerød Warming. Science 325, 310–314.
Mackintosh, A., Golledge, N., Domack, E., Dunbar, R., Leventer, A., White, D., Pollard, D., DeConto, R., Fink, D., Zwartz, D., Gore, D., Lavoie, C., 2011. Retreat of the East Antarctic ice sheet during the last glacial termination. Nature Geosci. 4, 195–202.
Marshall, S.J., James, T.S., Clarke, G.K.C., 2002. North American Ice Sheet reconstructions at the Last Glacial Maximum. Quat. Sci. Rev. 21, 175–192.
Obbink, E.A., Carlson, A.E., Klinkhammer, G.P., 2010. Eastern North American freshwater discharge during the Bølling-Allerød warm periods. Geology 38, 171–174.
Otto-Bliesner, B.L., Brady, E.C., 2010. The sensitivity of the climate response to the magnitude and location of freshwater forcing: last glacial maximum experiments. Quat. Sci. Rev. 29, 56–73.
Otto-Bliesner, B.L., Brady, E.C., Clauzet, G., Tomas, R., Levis, S., Kothavala, Z., 2006. Last glacial maximum and Holocene climate in CCSM3. J. Climate 19, 2526–2544.
Paterson, W.S.B., 1994. The Physics of Glaciers. Butterworth-Heinemann, Oxford. 480 pp.
Peltier, W.R., 1994. Ice age paleotopography. Science 265, 195–201.
Peltier, W.R., 2004. Global glacial isostasy and the surface of the ice-age Earth: the ICE-5G (VM2) model and GRACE. Ann. Rev. Earth Planet. Sci. 32, 111–149.
Peltier, W.R., 2005. On the hemispheric origins of meltwater pulse 1a. Quat. Sci. Rev. 24, 1655–1671.
Peltier, W.R., Fairbanks, R.G., 2006. Global glacial ice volume and Last Glacial Maximum duration from an extended Barbados sea level record. Quat. Sci. Rev. 25, 3322–3337.
Pollard, D., PMIP Participation Group, 2000. Comparisons of ice-sheet surface mass budgets from Paleoclimate Modeling Intercomparison Project (PMIP) simulations. Global Planet. Change 24, 79–106.
Poore, R.Z., Osterman, L., Curry, W.B., Phillips, R.L., 1999. Late Pleistocene and Holocene meltwater events in the western Arctic Ocean. Geology 27, 759–762.
Price, S.F., Conway, H., Waddington, E.D., 2007. Evidence for late Pleistocene thinning of Siple Dome, West Antarctica. J. Geophys. Res. 112, F03021. doi:10.1029/2006JF000725.
Rinterknecht, V.R., Clark, P.U., Raisbeck, G.M., Yiou, F., Bitnas, A., Brook, E.J., Marks, L., Zelcs, V., Lunkka, J.-P., Pavlovskaya, I.E., Piotrowski, J.A., Raukas, A., 2006. The last deglaciation of the southeastern sector of the Scandinavian ice sheet. Science 311, 1449–1452.
Severinghaus, J.P., Brook, E.J., 1999. Abrupt climate change at the end of the lasts glacial period inferred from trapped air in polar ice. Science 286, 930–934.
Shakun, J.D., Carlson, A.E., 2010. A global perspective on Last Glacial Maximum to Holocene climate change. Quat. Sci. Rev. 29, 1801–1806.
Smeets, C.J.P.P., van den Broeke, M.R., 2008. Temporal and spatial variations of the aerodynamic roughness length in the ablation zone of the Greenland Ice Sheet. Boundary Layer Meteorol. 128, 315–338.
Smith, J.A., Hillenbrand, C.-D., Kuhn, G., Larter, R.D., Graham, A.G.C., Ehrmann, W., Moreton, S.G., Forwick, M., 2011. Deglacial history of the West Antarctic Ice Sheet in the western Amundsen Sea Embayment. Quat. Sci. Rev. 30, 488–505.
Stanford, J.D., Rohling, E.J., Hunter, S.E., Roberts, A.P., Rasmussen, S.O., Bard, E., McManus, J., Fairbanks, R.G., 2006. Timing of meltwater pulse 1a and climate responses to meltwater injections. Paleoceanography 21, PA4103. doi:10.1029/2006PA001340.
Stokes, C.R., Tarasov, L., 2009. Ice streaming in the Laurentide Ice Sheet: a first comparison between data-calibrated numerical model output and geological evidence. Geophys. Res. Lett. 37, L01501. doi:10.1029/2009GL040990.
Stouffer, R.J., Yin, J., Gregory, J.M., Dixon, K.W., Spelman, M.J., Hurlin, W., Weaver, A.J., Eby, M., Flato, G.M., Hasumi, H., Hu, A., Jungclaus, J.H., Kamenkovich, I.V., Levermann, A., Montoya, M., Murakami, S., Nawrath, S., Oka, A., Peltier, W.R., Robitaille, D.Y., Sokolov, A., Vettoretti, G., Weber, S.L., 2006. Investigating the causes of the response of the thermohaline circulation to past and future climate changes. J. Climate 19, 1365–1387.
Sundal, A.V., Shepherd, A., Nienow, P., Hanna, E., Palmer, S., Huybrechts, P., 2011. Melt-induced speed-up of Greenland ice sheet offset by efficient subglacial drainage. Nature 469, 521–524.
Svendsen, J.I., Gataullin, V., Mangerud, J., Polyak, L., 2004. The glacial History of the Barents and Kara Sea Region. In: Ehlers, J., Gibbard, P.L. (Eds.), Quaternary Glaciations: Extent and Chronology. Elsevier, Amsterdam, pp. 369–378.
Svensson, A., Andersen, K.K., Bigler, M., Claussen, H.B., Dahl-Jensen, D., Davies, S.M., Johnsen, S.J., Muscheler, R., Parrenin, F., Rasmussen, S.O., Röthlisberger, R., Seierstad, I., Steffensen, J.P., Vinther, B.M., 2008. A 60,000 year Greenland stratigraphic ice core chronology. Clim. Past 4, 47–57.
Tarasov, L., Peltier, W.R., 2004. A geophysically constrained large ensemble analysis of the deglacial history of the North American ice-sheet complex. Quat. Sci. Rev. 23, 359–388.
Tarasov, L., Peltier, W.R., 2005. Arctic freshwater forcing of the Younger Dryas cold reversal. Nature 435, 662–665.
Tarasov, L., Peltier, W.R., 2006. A calibrated deglacial drainage chronology for the North American continent: evidence of an Arctic trigger for the Younger Dryas. Quat. Sci. Rev. 25, 659–688.
Todd, C., Stone, J., Conway, H., Hall, B., Bromley, G., 2010. Late Quaternary evolution of Reedy Glacier, Antarctica. Quat. Sci. Rev. 29, 1328–1341.
Weaver, A.J., Saenko, O.A., Clark, P.U., Mitrovica, J.X., 2003. Meltwater Pulse 1A from Antarctica as a Trigger of the Bølling-Allerød Warm Interval. Science 299, 1709–1713.
Zwally, H.J., Abdalati, W., Herring, T., Larson, K., Saba, J., Steffen, K., 2002. Surface melt-induced acceleration of Greenland ice-sheet flow. Science 297, 218–222.

Please cite this article as: Carlson, A.E., et al., Modeling the surface mass-balance response of the Laurentide Ice Sheet to Bølling warming and its contribution to Meltwater Pulse 1A, Earth Planet. Sci. Lett. (2011), doi:10.1016/j.epsl.2011.07.008